

# Spectrally Efficient Non-Orthogonal Multi-band CAP UDWDM Fiber-MMW Integration for 6G RAN Employing NN-Based Direct Waveform to Symbol Conversion

Jiang Chen<sup>1</sup>, Boyu Dong<sup>1</sup>, Junlian Jia<sup>1</sup>, Jianyang Shi<sup>1</sup>, Tao Li<sup>3</sup>, Chen Shen<sup>1,2</sup>, Junwen Zhang<sup>1,2\*</sup>, Nan Chi<sup>1,2\*</sup>  
<sup>1</sup>MoE Lab, Fudan University, Shanghai 200433, China, <sup>2</sup>Peng Cheng Lab, Shenzhen 518055, China, <sup>3</sup>STEC Lab, CSDDC, Wuhan 430000, China  
 \*junwenzhang@fudan.edu.cn, \*nanchi@fudan.edu.cn

**Abstract:** We propose a novel neural-network-based direct waveform-to-symbol conversion method in non-orthogonal multi-band CAP based UDWDM fiber-MMW integration system for 6G radio-access-network. Spectrally efficient fiber-MMW transmission is achieved at totally 384-Gbps capacity with 24 non-orthogonal sub-bands. © 2022 The Author(s)

## 1. Introduction

The six-generation mobile network (6G) is expected to delivery 1000x time more capacity compared with 5G, based on higher frequency spectrum to millimeter-wave (MMW) and much denser cell coverages [1]. To serve the high-speed transmission demand of 6G as well as the ultra-dense cell distributions, one of the key enablers is fiber-MMW integration network (FMMWIN) [2, 3]. FMWI simplifies the antenna site architecture of remote radio units (RRUs) in 6G radio access networks (RANs) by providing signals for MMW carrier modulation after photo-detection and amplification without any high-speed and high-complexity analog-to-digital converter (ADCs) or digital-to-analog converters (DACs) [3].

With the explosive increase of accesses, ultra-dense antennas will be arranged in densely populated areas. As shown in Fig. 1. (a), ultra-dense wavelength-division multiplexing (UDWDM) fiber-MMW integration based on multi-band carrierless amplitude and phase (m-CAP) can provide flexible wavelength-to-the-user and sub-band-to-the-user accesses with high data rate and low hardware complexity [4, 5]. In order to reach high spectral efficiency (SE), the wavelength spacing should be to as narrow as possible. Thus, it's necessary to compress the bandwidth of the signal in a UDWDM channel. As a candidate scheme for compressing signal bandwidth, non-orthogonal multi-band CAP (NM-CAP) reduces the spacing of adjacent sub-bands, leading to controllable inter-carrier interference (ICI) in the received symbols after matched filtering (MF). Wang et al. proposed a complex independent component analysis (ICA) algorithm based on subcarrier component extraction (SCE) to cancel ICI caused by overlapping of adjacent sub-bands [6, 7]. However, serious inter-symbol interference (ISI) makes SCE-ICA useless for canceling ICI. One simple approach to solve this problem is utilizing an LMS equalizer to cancel ISI before MF. However, the residual errors of LMS and MF lead to error accumulation, which will badly affect the performance of SCE-ICA.

In this paper, we propose and experimentally demonstrate a neural-network (NN)-based direct waveform-to-symbol conversion method in NM-CAP based UDWDM fiber-MMW integration system for 6G RAN. The NN-based waveform to symbol converter (NNWSC) directly converts the received NM-CAP waveform into QAM symbols, without the need for conventional CAP MFs, post-equalizers like LMS equalizer and ICI cancelation algorithms like SCE-ICA. NNWSC cancels the ISI and ICI simultaneously, simplifies the demodulation process and provides much better performances. Finally, spectrally efficient fiber-MMW transmission is achieved at totally 384-Gbps capacity with 24 NM-CAP-16QAM sub-bands on 8-UDWDM channels with 25-GHz spacing.

## 2. Principle of NM-CAP modulation and NNWSC based demodulation

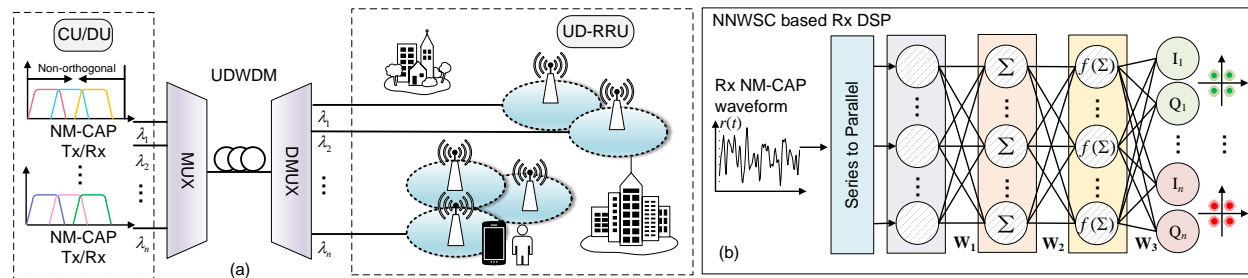


Fig. 1. (a) Conceptual diagram of FWMI. (b) Illustration of principle of NNWSC based DSP.

The generation of NM-CAP waveforms and the principle of NNWSC based DSP is shown in Fig. 1. At the beginning of NM-CAP modulation, binary data for multiusers is mapped to complex QAM symbols. Then the symbols are up-sampled and separated into in-phase (I) and quadrature (Q) signals for the next operation. The signals of per user are then filtered by a pair of Hilbert finite response filters (FIRs), which are called pulse shaping filters (PSFs). The most common way to generate the filters is to multiply square root raised cosine (SRRC) and cosine wave for I PSF and multiply SRRC and sine wave for Q PSF. The generated filters can be expressed by:

$$f_I^n(t) = g_{sq}(t) \cos(2\pi f_n t), \quad f_Q^n(t) = g_{sq}(t) \sin(2\pi f_n t), \quad (1)$$

where  $g_{sq}(t)$  is SRRC pulse,  $f_n$  is the center frequency of different sub-band for the  $n$ th user.  $f_n$  is denoted by  $f_n = (1 + \alpha)R_s/2 + (n - 1)\Delta f$ , where  $\alpha$  is the roll-off factor of SRRC pulse,  $R_s$  is the symbol rate, and  $\Delta f$  is the frequency spacing of adjacent sub-bands. When  $\Delta f \geq (1 + \alpha)R_s$ , all PSFs are orthogonal to each other. When  $\Delta f < (1 + \alpha)R_s$ , the adjacent sub-bands overlap each other, which will lead to inter channel interference (ICI).

At the receiver end, the received serial NM-CAP waveform data is converted to be parallel. The size of parallel data is equal to the input size of NN. Suppose the input data is denoted as  $\mathbf{x}(k)$ , then the output of NN can be expressed as

$$\mathbf{y}(k) = \mathbf{W}_3 f(\mathbf{W}_2(\mathbf{W}_1 \mathbf{x}(k) + \mathbf{b}_1) + \mathbf{b}_2) + \mathbf{b}_3, \quad (2)$$

where  $k$  represents the index of converted QAM symbols,  $\mathbf{b}_i$  ( $i=1, 2, 3$ ) denotes the bias of every NN layer,  $\mathbf{W}_i$  ( $i=1, 2, 3$ ) denotes the fully-connected weights which connect adjacent layers, and  $f(\cdot)$  denotes the activation function. Because matched filtering, LMS equalization and SCE-ICA are actually linear convolution, the specially designed NN structure can replace the function of them totally. Moreover, owing to the activation function, NNWSC can offset the nonlinear distortion. In this work, the nonlinearity in the system is weak, so the activation function is not used.

### 3. Experimental setup

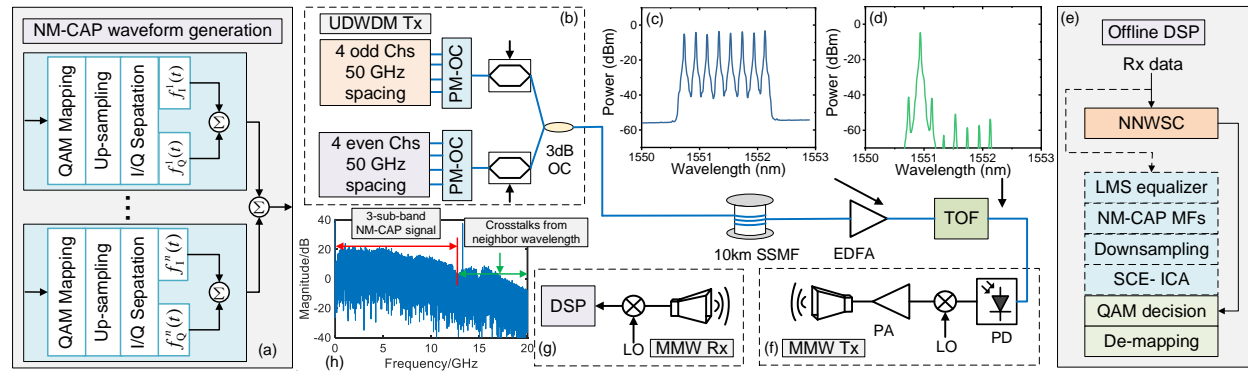


Fig. 2. Experimental setup and offline DSP (PM-OC: polarization-maintaining optical coupler; TOF: tunable optical filter; LO: local oscillator; PA: power amplifier; NNWSC: neural network based direct waveform to symbol conversion).

The setup of the UDWDM fiber-MMW integration system and the offline DSP is shown in Fig. 2. The UDWDM system includes 8 wavelengths with 25-GHz spacing and 14.5-dBm output power. Each of them is loaded with 3 NM-CAP sub-bands of 16 Gbps per user, 48 Gbps in total. In another word, the total transmission rate of the UDWDM system is 384 Gbps. At the transmitter end, the 8 wavelengths are divided into 2 groups, 4 odd wavelengths and 4 even wavelengths with 50 GHz spacing. The two groups of wavelengths are multiplexed by using polarization-maintaining optical couplers (PM-OCs) and the modulated by two different Mach-Zehnder modulators (MZMs) with different 3-sub-band NM-CAP data, respectively. The two branches of optical signals are coupled as one branch by a 3-dB optical coupler (OC) and then transmitted in a 10-km SSMF. Due to the coupling loss and fiber loss, the optical signal after 10-km transmission is amplified by an EDFA. At the receiver end of fiber link, the UDWDM optical signal is filtered by a tunable optical filter (TOF) and received by a photodetector (PD) in sequence. The electrical signal from PD is modulated to a 79-GHz mm-wave carrier, which is generated by multiplying 6 to a 13.167-GHz radio frequency using a  $\times 6$  active multiplier. The mm-wave signal is amplified by a power amplifier (PA) and transmitted by a horn antenna in sequence. The distance between the transmitter and the receiver is 1 m. At the receiver end of mm-wave link, the radio signal is demodulated by the local oscillator (LO), and then observed in a real time oscilloscope (OSC).

### 4. Experimental results

We firstly discuss the performance of a single wavelength without fiber in different cases. All figures in this section expect Fig. 4. (c) show the experimental results of the 2<sup>nd</sup> wavelength without fiber.

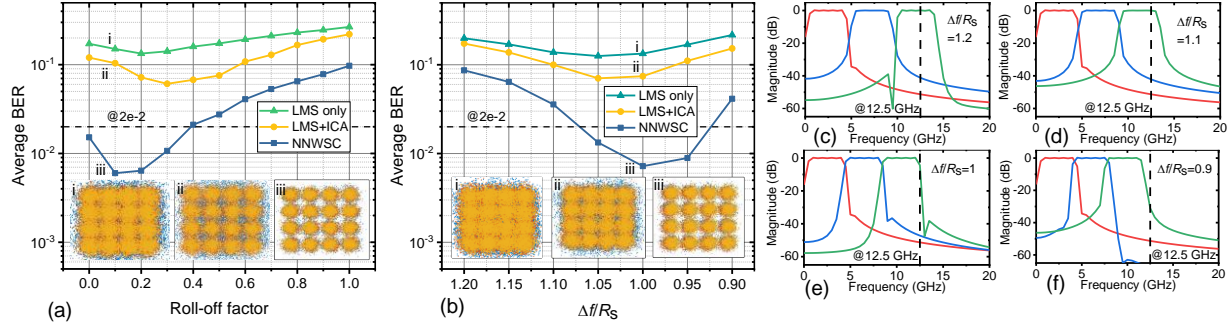


Fig. 3. (a) The relationship between BER and the roll-off factor of SRRC pulse in  $\Delta f/R_s = 1$  case; (b) the relationship between BER and the frequency spacing of adjacent sub-bands in  $\alpha = 0.2$  case; (c)~(f) the frequency responses of 3 PSFs in different frequency spacing cases.

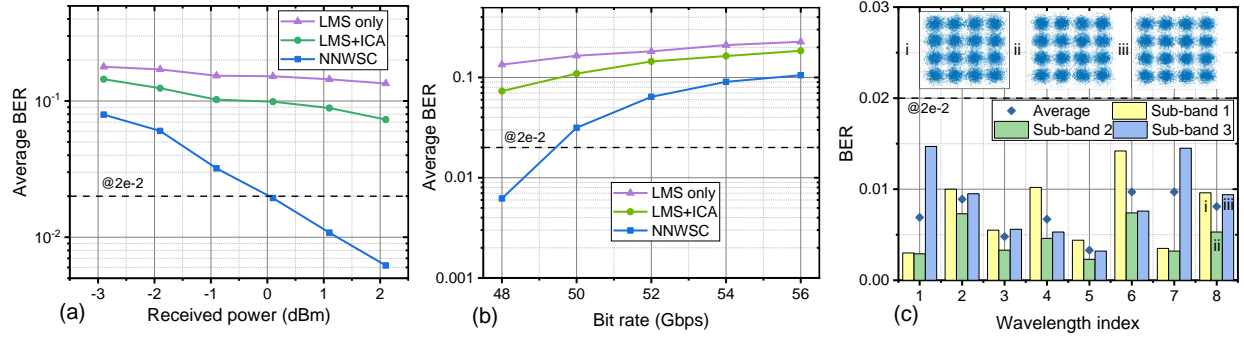


Fig. 4. (a) The relationship between BER and the received power; (b) The relationship between BER and total bit rate of the 2<sup>nd</sup> wavelength; (c) Average and every-sub-band BER of 8 UDWDM wavelengths after 10-km fiber transmission.

Fig. 3. (a) shows the relationship between BER and roll-off factor. The symbol length of SRRC pulse is 8. In the case of  $\alpha = 0$ , BER is higher because SRRC pulse decays slowly, leading to inherent ISI that can't be canceled. When  $\alpha > 0.2$ , the total bandwidth of 3-sub-band NM-CAP signal is more than 12.5 GHz, which is the half of the frequency spacing of adjacent WDM sub-channels, so BER becomes higher and higher. The average BER in  $\alpha = 0.1$  case is a little bit lower than that in  $\alpha = 0.2$  case, but BER of the first sub-band in  $\alpha = 0.1$  is much higher than that of the second sub-band and the third sub-band. Fig. 3. (b) shows relationship between BER and frequency spacing when  $\alpha = 0.2$ , Fig. 3. (c)~(f) show the frequency responses of 3 PSFs in different frequency spacing cases. In  $\Delta f/R_s = 1.2$  case, the total bandwidth is much higher than 12.5 GHz, so the BER in this case is highest. As the frequency spacing is lower, the total bandwidth becomes lower, which makes BER becomes lower. When the frequency spacing is too narrow, ICI caused by overlapping can't be canceled well. Fig. 4. (a) shows the relationship between BER and received optical power. As the received power increases, BER in all cases becomes lower. It's clear that the enhancement of the received power makes NNWSC benefit most. When the received power is 0.1 dBm, the average BER is below 20% overhead forward error correction (FEC) threshold of  $2 \times 10^{-2}$ ; when the received power is 2.1 dBm, the average BER is below  $1 \times 10^{-2}$ . As Fig. 4. (b) shows, the utmost bit rate of the 2<sup>nd</sup> wavelength is 48 Gbps, 16 Gbps per sub-band. Fig. 4. (c) shows the BER performance of all 8 UDWDM wavelengths, with 3 sub-bands per wavelength and totally 24 NM-CAP sub-bands. BER of all sub-bands is below  $2 \times 10^{-2}$ , average BER of all wavelengths is below  $1 \times 10^{-2}$ .

## 5. Conclusion

In this paper, an NNWSC method is proposed and demonstrated in UDWDM fiber-MMW integration system based on NM-CAP for 6G RAN. NNWSC simplifies the demodulation process and provides much better performances by converting the received NM-CAP waveform into QAM symbols directly. Finally, we achieve a spectrally efficient fiber-MMW transmission at totally 384-Gbps capacity with 24 NM-CAP-16QAM sub-bands on 8-UDWDM channels with 25-GHz spacing.

This work was partly support by the NSFC project (No.61925104, No.62031011, No. 62171137, No. 62071444), Shanghai NSF project (No. 21ZR1408700), Peng Cheng Laboratory project (No. PCL2021A14), and in part by the Fudan University-CIOMP Joint Fund.

## References

- [1] Y. Chen, et al., OFC 2021, paper Tu6E. 1.
- [2] M. Huang, et al., J. Lightwave Technol, 38, 1221-1229 (2020).
- [3] A. Delmade, et al., J. Lightwave Technol, 39, 465-474 (2021).
- [4] Y. Zhu, et al., J. Lightwave Technol, 37, 3875-3881 (2019).
- [5] J. Prat, et al., J. Lightwave Technol, 34, 783-791 (2016).
- [6] Z. Wang, et al, J. Lightwave Technol, 38, 6187-6201 (2020).
- [7] Y. Ha, et al, J. Lightwave Technol, 39, 4939-4950 (2021).